Influence of Ammonium Polyphosphate on the Mechanism of Thermal Degradation of an Acrylic Binder Resin

Christophe Drevelle,[1] Sophie Duquesne,[1] Michel Le Bras,[1] Jérôme Lefebvre,[1] René Delobel,[2] Andrea Castrovinci,[3] Carole Magniez,[4] Moïse Vouters[4]

[1]*Laboratoire des Procédés d'Elaboration de Revêtements Fonctionnels, UPRES EA 1040, ENSCL, BP 108, 59652 Villeneuve d'Ascq Cedex, France*
[2]*Centre de Recherche et d'Etude sur les Procédés d'Ignifugation des Matériaux, Parc de la Porte Nord, 62700 Bruay-la-Buissière, France*
[3]*Centro di Cultura per l'Ingegneria delle Materie Plastiche, V.T. Michel 5, 15100 Alessandria, Italy*
[4]*Institut Français du Textile et de l'Habillement, 59652 Villeneuve d'Ascq, France*

Received 23 December 2003; accepted 1 April 2004
DOI 10.1002/app.20868
Published online in Wiley InterScience (www.interscience.wiley.com).

ABSTRACT: The thermal behavior of an acrylic binder resin used in back coatings for textile applications was studied. The influence of the crystalline form of the fire-retardant additive on the thermal behavior was investigated. This resin formed a carbon char during its thermal degradation, so it may be assumed that it acts as a charring agent in intumescent systems with ammonium polyphosphate (APP) as the acid source. Thermogravimetric and spectroscopic analyses of acrylic binder resin/APP mixtures demonstrated the influence of the crystalline form of APP. The degradation mechanism of the binder resin could be described by ring closure and the formation of unsaturations. APP leads to the formation of a phosphocarbon structure that is thermally stable, whatever the crystalline form was of APP. © 2004 Wiley Periodicals, Inc. J Appl Polym Sci 94: 717–729, 2004

Key words: additives; degradation; flame retardance; resins; thermal properties

INTRODUCTION

Acrylic binder resins are used to coat fabrics[1] in many fields, including construction, transportation, and clothing. They allow the binding of fibers and the dispersion of additives, such as fire-retardant additives, on the surfaces of fabrics. This is particularly important because fabrics have to satisfy several fire tests, which are linked to their applications.

Two processes can be used to fire-retard synthetic fabrics: treatment of the bulk of the fiber (additives are placed in the polymer before the fiber is formed[2] or the polymer chain is modified) and surface modification of the fiber (coating[2]). One way of flame-retarding materials is using intumescent systems.[3–5] An intumescent system is generally composed of three active agents: an acid agent, a carbon source, and a blowing agent. Several successive reactions between these agents take place during the thermal degradation of the system and finally lead to the formation of a carbon expanded layer, which is generally called *char*. This char should be able to act as a thermal insulation shield for heat transfer from the flame to the polymer and as a physical barrier hindering the diffusion of volatiles toward the flame and of oxygen toward the polymer. As a result, the material is fireproofed.

The most common carbon sources are polyols such as penthaerythritol. Indeed, several studies in our laboratory have shown the efficiency of such intumescent systems.[6–9] However, polyols present some problems of solubility and exudation. An original and innovative way of achieving fire-retardant synthetic fibers by surface treatment is the use of a binder resin as a carbon source. Acrylic binder resins are usually used for the surface treatment of fabrics and could be an interesting source of carbon because of their ability to sometimes form a carbon layer when degraded.

An understanding of the mechanism of degradation is needed for us to improve fire-retardant systems. This article deals with the mechanism of degradation of a commercial acrylic binder resin and a mixture of a binder resin and ammonium polyphosphate (APP). In particular, the effects of the crystalline forms of fire-retardant additives on the interactions of additives and binder resins are examined.

Thermogravimetric analysis (TGA) was used to determine the characteristic steps of degradation and to study the interactions of fire-retardant additives with the polymer and their effects on the thermal stability of the system. Volatile degradation products and solid

Correspondence to: Sophie Duquesne (sophie.duquesne@ensc-lille.fr)

Contract grant sponsor: NEREFITE; contract grant number: G1RD-CT-2001-00579.

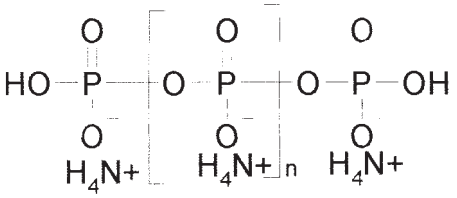

Figure 1 Schematic formula of APP.

residues at determined heat-treatment temperatures (HTTs) were then analyzed with Fourier transform infrared (FTIR) and solid-state NMR, respectively, to obtain a better understanding of the mechanism of degradation of the binder resin/APP mixture.

EXPERIMENTAL

Materials

The raw materials were an acrylic binder resin[1] (Repolem 1122 TK, Atofina), in the form of an emulsion of the polymer, and APP (Fig. 1) crystalline form I (Antiblaze MC, Rhodia, Paris, France; soluble fraction in H_2O = 2.77 wt %) and APP crystalline form II (Exolit 422, Clariant; soluble fraction in H_2O < 1 wt %).

The characteristics of the acrylic binder resin (aqueous emulsion) are given in Table I. The crystalline forms of APP[10] differ in their chain size. Form I contained chains with average sequences of tetrahedral PO_3^- that were much shorter than those of form II (Fig. 1).

The APP/resin mixture was obtained with the following procedure. First, APP was dispersed in water, and then an acrylic emulsion was added (10 wt % APP, 45 wt % water, and 45 wt % acrylic emulsion). This mixture was mixed with an Ultra Turax rotor/stator system (Mac Technologie; Gretz-Armainvilliers, France) at 8,000 rpm for 8 min and then at 13,500 rpm for 2 min.

APP/resin films (Table II) were obtained by the wet mixture being placed in an aluminum pan covered with Teflon and being dried at 90°C until a constant weight was obtained. It was dried again at 150°C for 2 min to eliminate residual water and to reticulate the films.

X-ray diffraction (XRD)

All the samples were powders and were examined under the same experimental conditions with a Siemens 5000 diffractometer. Copper radiation was used, and the applied voltage was 40 kV with a 25-mA current ($\lambda_{Cu\ K\alpha}$ = 1.54 Å). A graphite monochromator was used to produce Kα radiation. A 2θ scan was made from 10 to 45° at 0.8°/min in a Bragg–Brentano configuration ($2\theta/\theta$).

With the Joint Comittee Powder Diffraction Standards-International Centre for Diffraction Data (JCPDS-ICPD) database, the crystalline phases were identified from their observed XRD patterns.

TABLE I
Characteristics of Repolem 1122 TK Acrylic Binder Resin

Vitreous temperature T_g (°C)	Solid content (%)	Stabilization	pH	Viscosity (mPa.s)
2	59–61	Anionic and nonionic	7–8	100–350

TABLE II
Compositions of Different Dried Films

Dried film	APP (wt%)	Binder resin (wt%)
Acrylic binder resin	0	100
Acrylic binder resin + APP I	25	75
Acrylic binder resin + APP II	25	75

FTIR spectroscopy

FTIR spectra of the films were obtained with a Nicolet 400D (Access IR, Brémoncourt, France) device from 700 to 4000 cm^{-1}. A purge system (Lab Gas) was used for scanning under dried air without carbon dioxide. Sixty-four scans were made at a resolution of 4 cm^{-1}.

The films (virgin binder resin or a mixture of the additives and binder resin) were analyzed with an attenuated total reflection system, and the residues were ground and mixed with KBr to form pellets for transmission analysis.

Scanning electron microscopy (SEM)

The fracture surfaces in liquid nitrogen of the samples were studied with a JEOL JSM T330 A scanning electron microscope (JEOL; Croissy sur Seine, France). The samples were mounted on an aluminum stub with double-sided tape and then gold-coated with a JEOL Ion Sputter JFC-1100 coating unit to prevent electrical charging during the examination.

TGA

TGA was performed at 10°C/min under synthetic air (flow rate = 0.75×10^{-7} m^3/s, Air Liquid grade) with

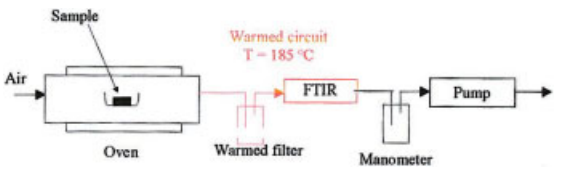

Figure 2 Schematic diagram of the tubular furnace coupled with an FTIR spectrometer.

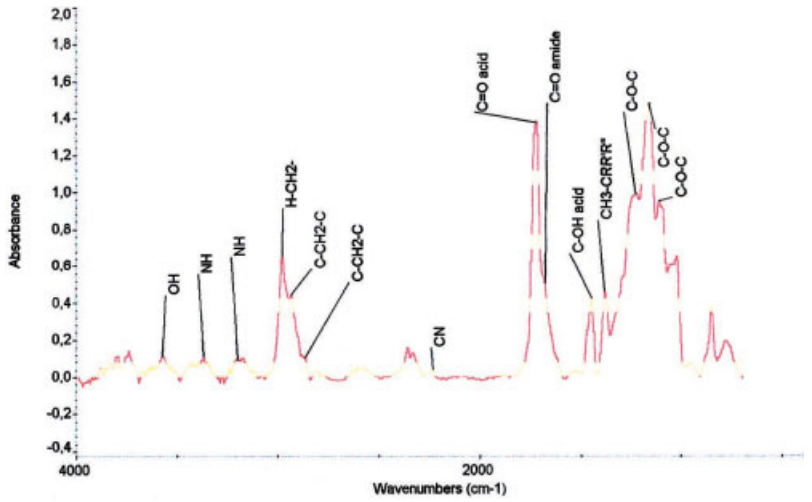

Figure 3 IR spectra of the pure acrylic binder resin.

a Setaram 92-16/18 microbalance. The sample weight was fixed at 10 mg, and the sample was positioned in open vitreous silica pans. The precision of the temperature measurements was 1.5°C over the whole temperature range.

The curves of the weight differences between the experimental and expected TGA curves were computed as follows:

$$\Delta[M(T)] = M_{\text{exp}}(T) - M_{\text{theo}}(T)$$

where $\Delta[M(T)]$ is the curve of the weight difference, $M_{\text{exp}}(T)$ is the TGA curve of the fire-retardant material (resin/APP), and $M_{\text{theo}}(T)$ is the TGA curve computed by a linear combination of the TGA curves of the APP and binder resin:

$$M_{\text{theo}}(T) = \sum_{1} \%i \times M_i(T)$$

where $\%i$ is the weight percentage of material i in the initial material and $M_i(T)$ is the residual weight of material i at temperature T. The $\Delta[M(T)]$ curve enabled the observation of an eventual increase or decrease in the thermal stability of the polymer related to the presence of the additive. Synergistic effects were represented by a positive $\Delta[M(T)]$ value represents a synergistic effects, and a negative $\Delta[M(T)]$ value represents antagonistic effects.

Thermal degradation

Experiments were carried out at different characteristic HTTs (250, 370, 430, and 490°C) for 20 min. In all cases, the sample mass was fixed at about 3 g. The samples were positioned in open pans placed in a tubular furnace.

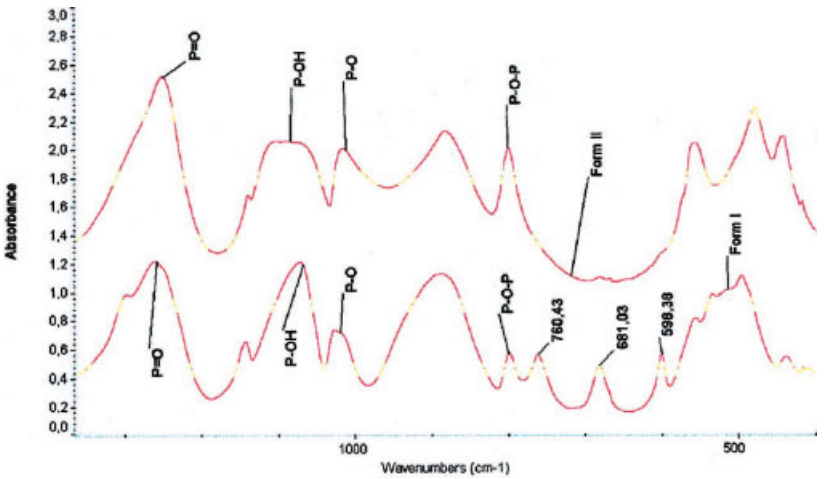

Figure 4 FTIR spectra of both crystalline forms of APP.

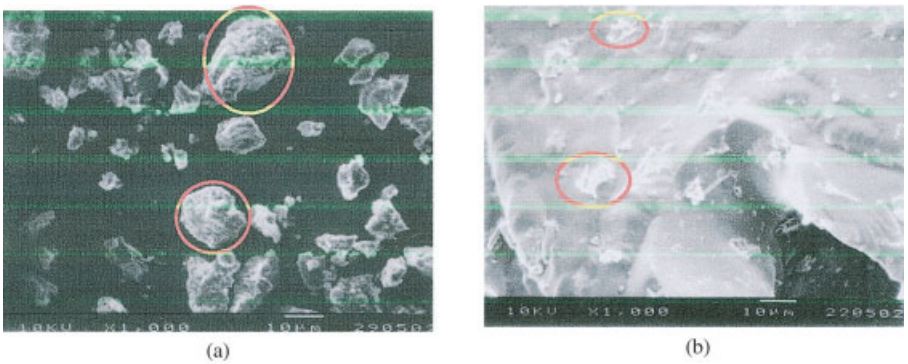

Figure 5 Particle size of crystalline form I (SEM images, original magnification = 1000×): (a) dry particles and (b) dried film.

Analyses of the gases

Qualitative analyses: FTIR

Gases were continuously evacuated with a pump (2 L/min). A Nicolet 710C FTIR spectrophotometer was placed online and enabled the continuous detection of gas components in smoke (Fig. 2).

The gas cell had a volume of 750 cm^3 and a 3.77 m path length and was operated at 650 Torr. The sampling line was maintained at 185°C. Therefore, the partial pressure of the combustion products could be low enough to prevent liquid or solid condensation in the sampling line and in the cell. The FTIR instrument was set to generate one spectrum every 9 s.

Quantitative analyses: HCN measurements

The tubular furnace method (norm NFX 70-100) allows the thermal degradation under air of polymer materials associated with a quantitative analysis of the combustion gases (CO_2, CO, HCN, and SO_2).

Experiments were carried out at 600°C for 20 min. In all cases, the sample mass was fixed at about 1 g. The samples were positioned in open pans placed in a tubular furnace. Gases were continuously evacuated with a pump (0.12 m^3/h).

In this study, the evolved quantity of cyanhydric acid during the degradation of the samples was determined. This acid was collected in traps (in NaOH 0.1 mol/L). The concentrations of the solutions were then determined with ionic chromatography.

Analyses of the residues: solid-state NMR

Cross-polarization (CP)/dipolar decoupling (DD)/magic-angle-spinning (MAS) ^{13}C solid-state NMR analyses were performed on residues of the thermal degradation at characteristic HTTs.

Spectra were taken with a Bruker ASX 100 spectrometer (7-mm probe). The frequency was 25.2 MHz, and MAS, DD, and CP were used. The Hartmann–Hahn conditions for CP were obtained through the regulation of the canal power of the protons for maximum free induction decay of the ^{13}C adamantane signal.

One thousand scans were taken to obtain a good signal/noise ratio. The time between each scan was 5 s. The rotation speed was 5 kHz. The reference for the chemical shifts was tetramethylsilane. The contact time was 1 ms under Hartmann–Hahn conditions.

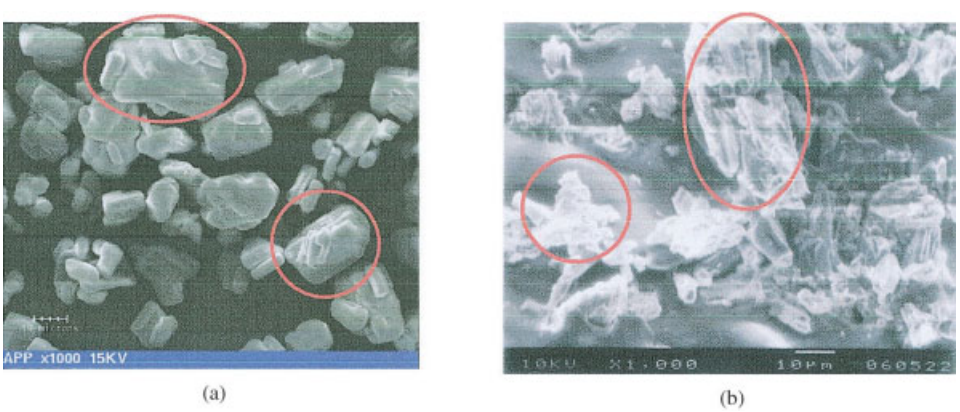

Figure 6 Particle size of crystalline form II (SEM images, original magnification = 1000×): (a) dry particles and (b) dried film.

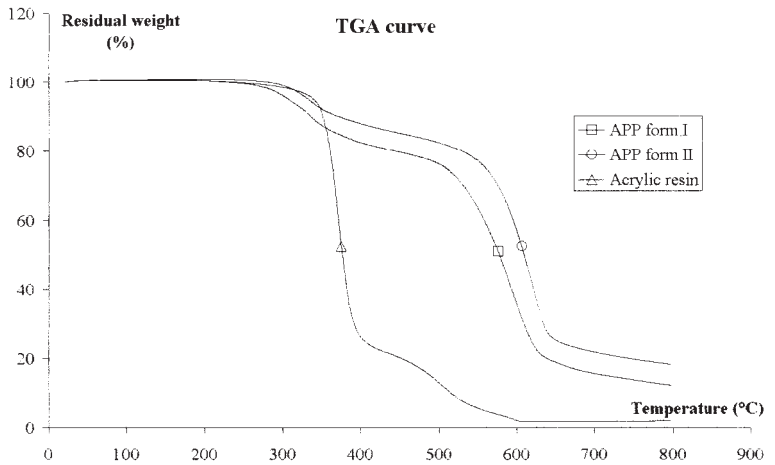

Figure 7 TG curves of raw materials at 10°C/min under air.

RESULTS AND DISCUSSION

Characterization of the raw materials

Acrylic binder resins are produced by the radical polymerization of different monomers. The monomers used in the manufacture of Repolem resin are acrylic acid, methacrylic acid, acrylonitrile, acrylamide, and acrylic ester (with a C8 ester chain at the maximum; Fig. 3).

FTIR spectra of both forms of APP show the presence of peaks corresponding to phosphates and ammonium: at about 1250 cm^{-1} for P═O bonds and at 1010 and 1060 cm^{-1} for P—O bonds (Fig. 4). The band at 800 cm^{-1} characterizes the bond P—O—P. Moreover, the characteristic peaks of form I at 760, 680, and 602 cm^{-1} are absent in the spectrum of form II.[11]

XRD shows that crystalline form I contains some impurities, unlike crystalline form II. The impurities are ammonium carbonate and ammonium hydrogen phosphate.[10,12]

Crystalline form II has an orthorhombic structure (a = 4.256 Å, b = 6.475 Å, and c = 12.04 Å) in the $P2_12_12_1$ spatial group. Form I has an orthorhombic structure with a = 14.50 Å, b = 21.59 Å, and c = 4.85 Å.

The particle size depends on the crystalline form. The particles of form I are 10–20 μm in size, as described in the literature[13] [Fig. 5(a)]. The particle size of form II is about 10–40 μm [Fig. 6(a)].

The particle size of form I is different in dried films, being less than 10 μm [Fig. 5(b)], although form II seems to maintain its particle size [Fig. 6(b)]. During the dispersion of crystalline form I in the acrylic binder resin, the particle size decreases, whereas form II particle size remains the same. This may be reasonably explained by the fact that form I has a shorter chain length and is thus more sensitive to water (soluble fraction in H_2O = 2.77 wt %; it is less than 1 wt % for form II). As the acrylic binder is water-based, the water partially solubilizes form I.

Thermostability of the raw materials and products

The degradation of APP I and APP II occurs in two steps (Fig. 7 and Table III). The first stage corresponds

TABLE III
Different Information from the TGA Curves of the Different Samples (% in Dry Samples)

Step	Temperature	Resin	APP I	APP II	Resin + APP I	Resin + APP II
1	Onset (°C)	285	270	300	245	255
	Maximum (°C)	370	335	335	365	370
	End (°C)	440	450	460	430	440
	Residual weight (%)	22	80	85	50	50
2	Onset (°C)	440	450	460	430	440
	Maximum (°C)	500	590	620	720	730
	End (°C)	580	800	800	800	800
	Residual weight (%)	7	12	18	10	11
3	Onset (°C)	580				
	Maximum (°C)	590				
	End (°C)	610				
	Residual weight (%)	2	—	—	—	

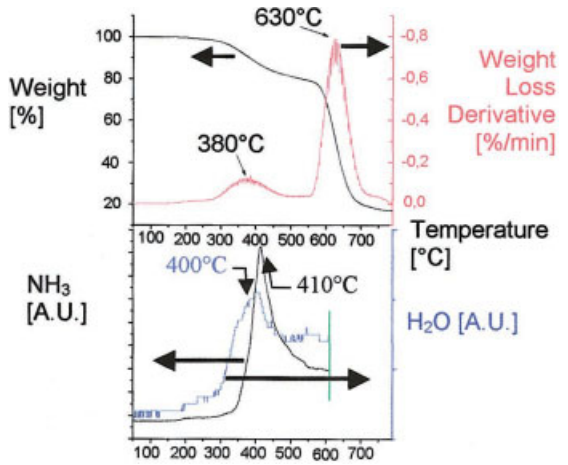

Figure 8 FTIR–TG curves of APP II at 20°C/min under nitrogen.

to a weight loss of 15% for APP II and of 20% for APP I. The higher first weight loss of form I may be attributed to the presence of impurities (urea) due to the mode of preparation of form I. Form I is prepared through the heating of an equimolar mixture of ammonium orthophosphate and urea under a blanket of anhydrous ammonia at 280°C.[12] Form II is obtained from the heating of form I, so no urea may be present.[12]

The second step presents the maximum weight loss at 590 and 620°C for APP I and APP II, respectively. The thermal behavior depends on the crystalline form. The degradation mechanisms of APP have already been studied in the literature.[14] The first step, which starts at about 300°C, corresponds to the release of ammonia and water (Fig. 8). The crosslinked phosphoric acid forms condensed species. During the second step, which occurs at about 550°C, the evaporation of phosphoric acid and the dehydration of the acid in P_4O_{10}, which sublimates, are thought to occur. Moreover, the final residual weight differs: form II has a bigger residual weight (18.2%) than form I (12.2%).

It has been previously demonstrated that under nitrogen, APP I is thermally weaker than APP II. However, under an inert atmosphere, the same final residual weight has been reached.

The pure acrylic binder resin shows three degradation steps (Table III and Fig. 7). The major step of degradation presents a maximum rate of degradation at 370°C with a 78% weight loss.

The second step presents a maximum weight loss of 15% at 500°C, and the third presents a maximum weight loss of 5% at 590°C. At the end of degradation, the residual mass is 2%.

When APP is added to the acrylic binder resin, the thermal stability of the binder is strongly modified (Fig. 9 and Table III). Both crystalline forms of APP stabilize the structure from 380 to 800°C. The major degradation step presents a maximum rate of degradation at 365–370°C (with a 50% weight loss vs a 78% weight loss for the pure resin). Then, the material degrades slowly between 380 and 680°C. Finally, a second step of degradation is observed at a higher temperature (25% weight loss at the maximum rate of degradation) and leads to the formation of a stable residue (ca. 10%). As a result, the degradation mechanism of the binder resin is modified by the addition of APP. Chemical reactions between the APP and resin should occur and lead to a thermally stable structure.[3–5] This is clearly shown by the curves of the weight difference, which put forward eventual interactions between the APP and binder resin (Fig. 10).

First, these curves demonstrate that there is no difference between the crystalline forms of APP. The temperature range in which the interactions of the additives and binder lead to the stabilization of the material is 380–800°C. A destabilization of the material is observed between 270 and 370°C. This can prob-

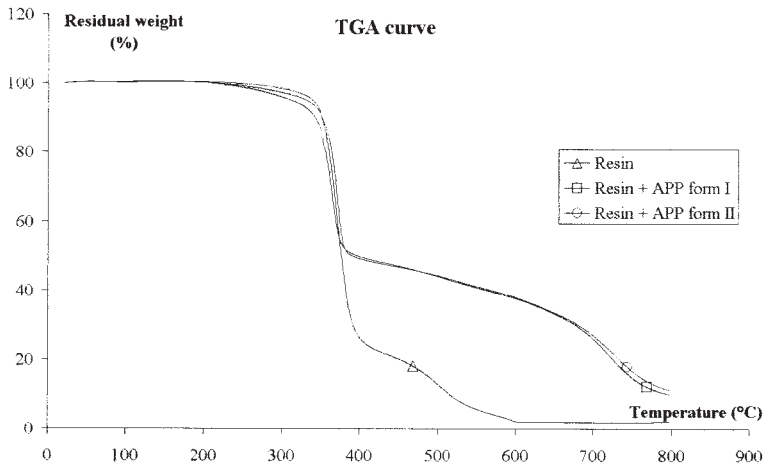

Figure 9 TG curves of dried films.

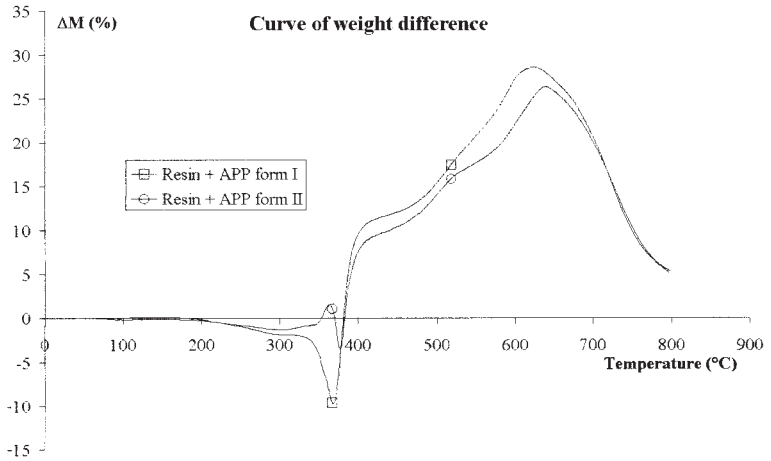

Figure 10 Curves of the weight difference for treated resins.

ably be attributed to a catalytic action of degradation of H_3PO_4 (formed during the degradation of APP) on the binder resin, as previously observed in polyurethane and Ethylene Vinyl Acetate copolymer (EVA), for example.[3,6–8,13–15]

In conclusion, the addition of APP to the binder resin leads to the following:

- small reduction of the onset temperature of degradation of the system.
- the formation of a thermally stable material, which is important in an intumescent system because it is this shield that acts as a protective barrier.

These conclusions have been observed for both crystalline forms of APP.

Characterization of the volatile degradation products and residues

To better understand the mechanisms of degradation of the binder resin and the mixture of the binder resin and APP, we determined four characteristic temperatures (HTTs) were determined from thermogravimetry (TG) curves (Fig. 11 and Table IV) to simulate the degradation steps of the resin and the mixture,

- 250°C corresponds to the beginning of the first step of degradation for the binder resin and for the mixture,
- 370°C corresponds to the beginning of the second step of degradation for the pure resin and for the mixture,
- 430°C represents the end of the second step of degradation for the pure resin and an intermediate step of the degradation for the FR mixture,
- 490°C corresponds to the end of the degradation for the pure binder resin and to an intermediate step of the degradation for the FR mixture.

Volatile degradation products

Figure 12 presents the spectra of the gases that evolved at 370°C for the mixture of the resin and APP II. Table V shows the degradation gases that

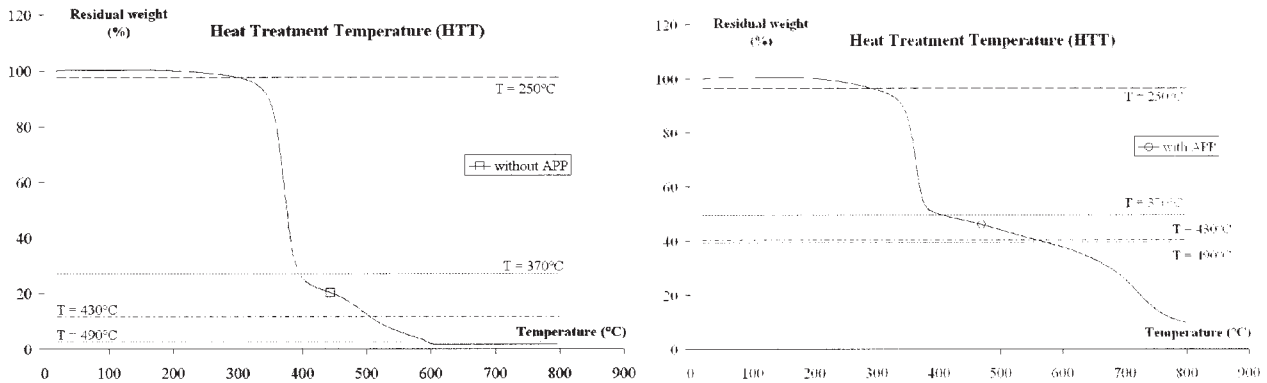

Figure 11 Determination of the characteristic degradation temperatures for a resin/APP mixture and the pure resin.

TABLE IV
Description of Isothermally Heat-Treated Samples

Product	HTT (°C)	Residual weight (%)	Product	HTT (°C)	Residual weight (%)	Product	HTT (°C)	Residual weight (%)
Acrylic resin	250	97.7	Acrylic resin+ APP I	250	95.9	Acrylic resin+ APP II	250	96.4
	370	30.3		370	48.9		370	49.7
	430	10.8		430	42.4		430	40.3
	490	2.5		490	37.1		490	39.5

evolved during the degradation of the different samples. First, the degradation of the pure resin occurs through the release of methanol, carbon dioxide, carbon monoxide, water, and a compound with an amide function ($-\overset{O}{\overset{\|}{C}}-NRR'$). At higher temperatures, cyanhydric acid, methane, alkene and aldehydes can be observed.

Films containing APP release ammonia at the beginning of degradation, and no aldehydes are present. No cyanhydric acid can be detected in the resin/APP system. Two assumptions can be proposed: first, the signal is too weak (too little acid to be detected) and second, the signal is hidden by one of the ammonia (harmonic at 3450 cm^{-1}) and a broad peak of C—H (═C—H and —C—H at 3200–3000 cm^{-1}). The norm NFX 70-100 allows us to determine if the presence of APP limits the formation of cyanhydric acid (Table VI). As the dispersion of this method is about 15%, the results show that the presence of APP does not limit the formation of cyanhydric acid. Therefore, the signal is hidden by those of ammonia and C—H bonds.

The crystalline form does not modify the nature of the degradation gases.

Residues

^{13}C-NMR spectra of residues of degradation containing APP I are similar to those of residues with APP II (Figs. 13–15).

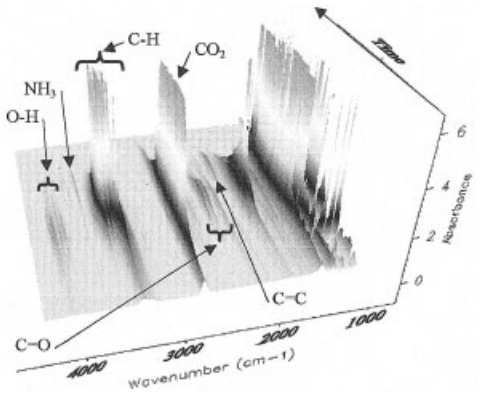

Figure 12 IR spectra of degradation gases at 370°C for APP II/resin mixtures versus time.

At 250°C, there is no evidence of degradation of the pure resin (Fig. 13 and Table VII). At this temperature, the degradation has not yet occurred (Table IV and Fig. 11): there is 98% residue. However, the detection of gases with an FTIR spectrometer (Table V) implies that degradation has begun.

At 370°C, the degradation of the pure acrylic resin occurs, and a peak at about 126 ppm appears. This peak corresponds to C═C and C═N bonds (aromatics and alkenes). Moreover, the carbonyl peak disappears, and it may be assumed that the first step of degradation of the resin corresponds to the degradation of carboxylic and amide functions.

The ^{13}C spectra of formulations with APP, crystalline form I or II have, (not presented in the paper) have the same aspects at 430 and 490°C than the one of the pure binder resin.

At 430 and 490°C, the peaks at 30–50 ppm (tertiary, secondary, and primary carbons) disappear. Only the peak at 126 ppm remains (C═C and C═N unsaturations). It may be proposed that the condensation and oxidation of the structure occur in agreement with a broadening of this peak.[15]

The FTIR analyses of the degradation residues show that APP (form I or II; there is no difference between the forms) has an impact (Fig. 16 and Table VIII) on the degradation of the resin. Ester and amide functions disappear, and an imide function ($-\overset{O}{\overset{\|}{C}}-\underset{H}{N}-\overset{O}{\overset{\|}{C}}-$) appears (at 250 and 370°C, respectively). If APP is added, the residue is a dense carbon solid with a structure that is not very friable in comparison with samples without APP.

Concerning the degradation of the pure acrylic resin, carboxyl acid functions (1733 cm^{-1}) and amide functions (1717 cm^{-1}) disappear progressively and imide functions (1725 cm^{-1}) appear.

Ether functions (C—O—C bonds) also disappear (1250–1100 cm^{-1}), and a new peak of C—O—C bonds appears in the same wave-number range: probably the ether function of anhydride.

Peaks of alcohol and amide functions (O—H and N—H) disappear, and peaks of C═C, C═N unsaturations appear during the thermal degradation.

For the mixture with APP, the degradation is accelerated: at 370°C, only broad peaks remain that are due to C═C and C═N aromatic bonds and P—O—C

TABLE V
Summary of Significant IR Absorbances of Gases of Degradation[16]

Species	Absorption bands (cm^{-1})	Assignment	Resin				Resin + APP crystalline form I				Resin + APP crystalline form II			
			T = 250°C	T = 370°C	T = 430°C	T = 490°C	T = 250°C	T = 370°C	T = 430°C	T = 490°C	T = 250°C	T = 370°C	T = 430°C	T = 490°C
NH_3	3400–3200	N—H stretching					X	X	X	X	X	X	X	X
	1620	Asymetric deformation					X	X	X	X	X	X	X	X
CH_3OH	3700–3100	Free and bond O—H stretch	X	X	X	X	X	X	X	X	X	X	X	X
	2900–2880	H—CH_2OH stretching	X	X	X	X	X	X	X	X	X	X	X	X
	1500–1400	CH_3—OH stretching	X	X	X	X	X	X	X	X	X	X	X	X
HCN	3405–3210	C—H stretching		X	X	X								
CH_4	3200–2850	Asymmetrical stretching			X	X	X	X	X	X		X	X	X
	1310	Bending			X	X				X				X
CO_2	2400–2250	Asymmetrical stretching	X	X	X	X	X	X	X	X	X	X	X	X
CO	2250–2000	C═O stretching	X	X	X	X	X	X	X	X	X	X	X	X
Aldehyde	2900–2700	C═O stretching			X	X								
Amide	1790–1720	C═O stretching	X	X	X	X		X	X	X		X	X	X
Alkene	3200–2950	C—H stretching		X	X	X		X	X	X		X	X	X
	1680–1620	C═C stretching		X	X	X		X	X	X		X	X	X
	1410	CH_2 in-plane deformation		X	X	X		X	X	X		X	X	X
Water	1800–1400	O—H blend	X	X	X	X	X	X	X	X	X	X	X	X

T = temperature.

TABLE VI
HCN Amounts in the Different Samples

Sample	HCN (mg/g)	Variation in comparison to the resin (%)
Resin	6.88	0
Resin + APP I	7.86	14.3
Resin + APP II	7.33	6.5

bonds (Table VIII), in agreement with what was previously proposed according to TGA. All the peaks present for the pure resin disappear. The thermally stable structure presents a broad peak at 1100–1300 cm^{-1}. This peak comes from the formation of bonds between the APP and carbon structure (P—O—C bonds).[3] The formation of such species has already been proposed as a partial explanation for the fire-retardant mechanism. Indeed, it leads to the following:

- a thermal stabilization of the material acting as a protective barrier,
- a deformation of the structure rather than crack formation.[15,18,19]

Discussion

TGA shows that the addition of APP to an acrylic resin enables the formation of a thermally stable structure during degradation, whatever the crystalline form is of the fire-retardant additives. First, concerning the degradation of the pure resin, ^{13}C-NMR shows the appearance of C═C and C═N unsaturations (126 ppm) and the disappearance of carboxylic functions of esters (174 ppm) to the benefit of anhydride functions and imide functions (160 ppm). Moreover, imide functions and amide functions are detected in the gas phase. As a result, it may be proposed that ring closure of polymer chains occurs and leads to the forma-

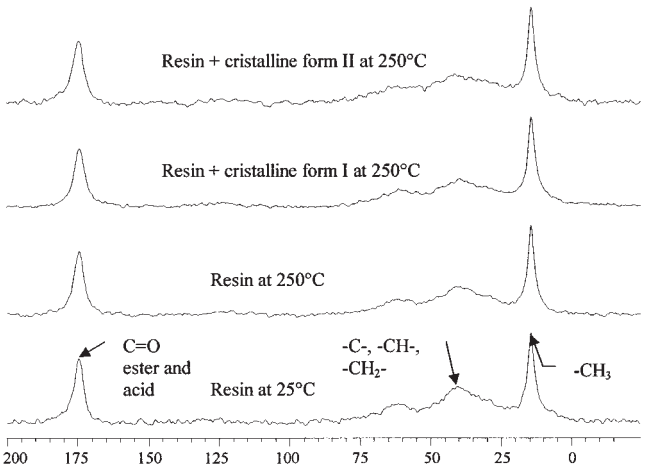

Figure 13 ^{13}C-NMR spectra of degradation residues for three mixtures at 250°C and the pure resin at 25°C.

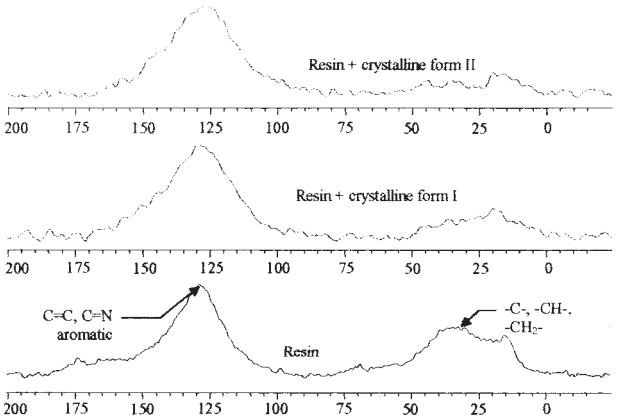

Figure 14 ^{13}C-NMR spectra of degradation residues for the materials at 370°C.

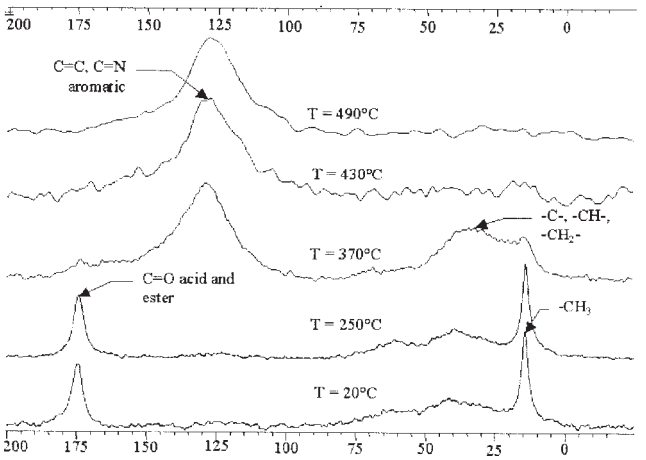

Figure 15 ^{13}C-NMR spectra of degradation residues for the pure resin at different degradation temperatures.

tion of cyclic anhydride and imide, as already proposed in literature[20–30] and as illustrated in eqs. (1) and (2).[29,30] FTIR analyses support this hypothesis because the anhydride function and imide function and C═C, C═N unsaturations appear, whereas amide, cyano, carboxylic, and ester functions disappear, when the HTT increases.

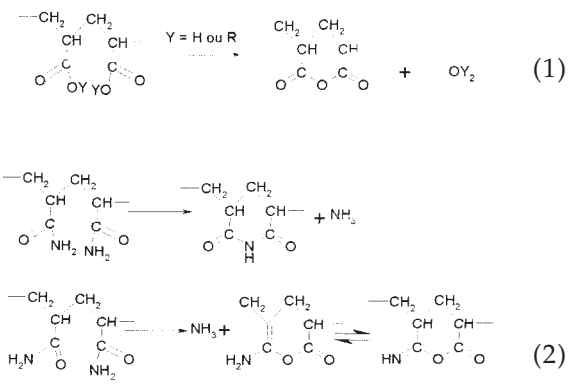

(1)

(2)

Ring closure occurs with the release of small molecules: water, ammonia, ether, and alcohol.[20–30] These gases have been detected during the thermal degradation and confirm this hypothesis.

On the basis of these results and those reported in the literature,[20–33] several mechanisms are postulated for the thermal degradation of the studied acrylic resin.

The anhydride is formed with the elimination of water, alcohol, or ether, which depends on the sequence of the polymer motif. For example, if R is an ethyl group, then diethyl ether is formed. Two other cycles can be formed with the elimination of ammonia: an imide function ( ) or function [eq. (2)], which is detected in the gas phase. For the pure resin, the ammonia signal, which comes from amide functions of the resin, is not detected. Two assumptions can be proposed:

- the signal is hidden by harmonics of cyanhydric acid,
- ammonia is trapped in the carbon structure, which is formed during thermal degradation.

C═N unsaturations can be formed with different possibilities because of amide functions [eqs. (2)–(4)]:

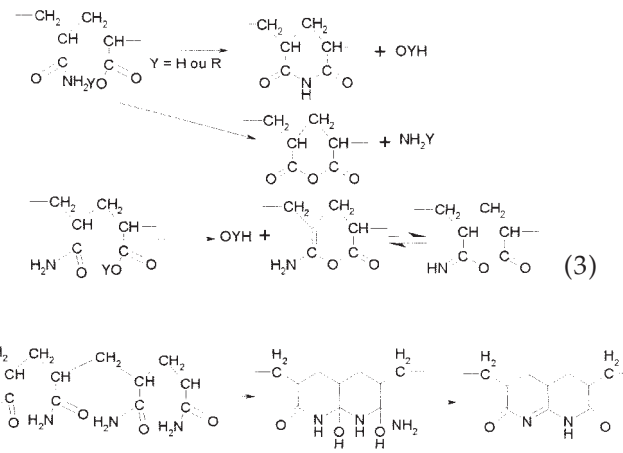

(3)

(4)

TABLE VII
NMR Peak Values for the ^{13}C-NMR[17] of the Degradation Residues

Peak (ppm)	Carbon
174	C═O acid–ester
160	C═O anhydride, imide
126	C═C, C═N aromatic
60	—C—O—
30–50	R_2—C—R_2, R—CH—R_2, R—CH_2—R
14	—CH_3

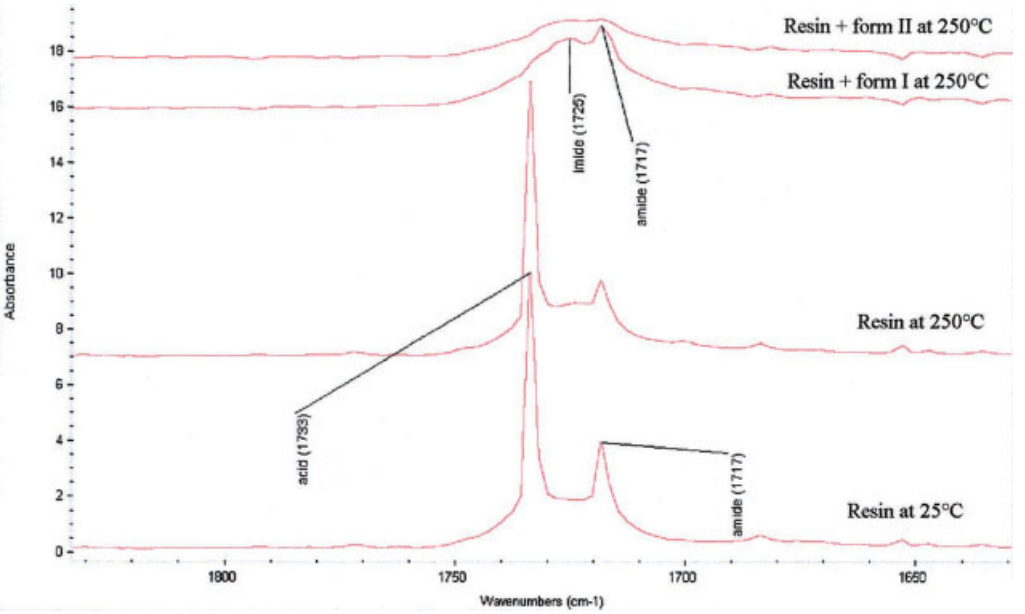

Figure 16 IR spectra of degradation residues.

All these ring closures depend on the polymer motif. Therefore, the previous gases are not detected, either because of the polymer motif or because of the kinetics of the reactions.

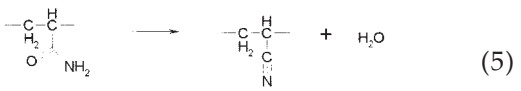

(5)

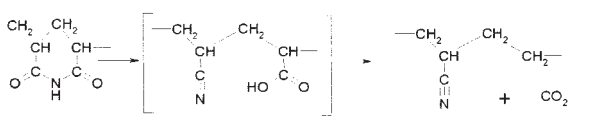

(6)

The degradation of the amide functions allows some nitrile functions to be formed [eqs. (5) and (6)].[29,30] The nitrile functions, along with the intrinsic nitrile functions by thermal degradation, eliminate cyanhydric acid and form C═C unsaturations.[31,32]

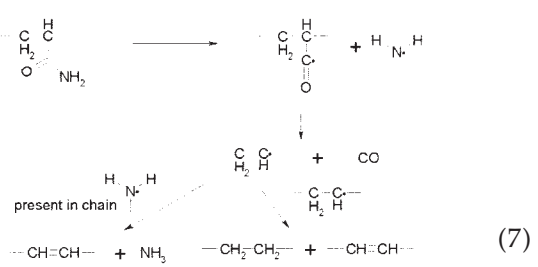

(7)

These C═C unsaturations can be formed with radical reactions [eq. (7)].[25,33] This mechanism can be considered with carboxylic acid and ester functions ($OH^{\bullet}$ radicals and $RO^{\bullet}$ radicals, respectively). This is the case for methyl methacrylate, which is present in the polymer motif, with $CH_3O^{\bullet}$.[25,33] C═C unsaturations also come from chain breaking mechanisms with proton transfers (intramolecular or intermolecular).

All these mechanisms occur nearly at the same time: they are linked to the polymer motif, the kinetics of the reactions and the temperature.

As for the degradation of resin/APP system, the addition of APP leads to the formation of a more thermally stable system. This effect does not depend on the crystalline form. APP is degraded to form phosphoric acid. This acid catalyzes the degradation of the resin and leads to a phosphocarbon structure that is more stable thermally.

CONCLUSIONS

The addition of APP to the studied acrylic resin leads to the formation of a more thermally stable structure. The mechanism of protection comes from the formation of a thermal barrier, which is observable after thermal degradation; there are no friable solid residues. This barrier is made of phosphocarbon and aromatic compounds and is formed rapidly: APP is degraded in phosphoric acid and then catalyzes the degradation of the resin to form the barrier.

The mechanisms described in the literature agree with the different results (the spectra of residues and gases) and show the formation of cycles, which are formed during the aromatic degradation cycles. These aromatic cycles are needed to form the shield. No

TABLE VIII
Summary of Significant IR Absorbances of Degradation Residues[16]

Species	Absorption bands (cm^{-1})	Assignment	Resin			APP I	APP II	Resin + APP crystalline form I			Resin + APP crystalline form II			
			T = 25°C	T = 250°C	T = 370°C	T = 25°C	T = 25°C	T = 25°C	T = 250°C	T = 370°C	T = 25°C	T = 250°C	T = 370°C	T > 370°C
O—H	3700–3100	Stretch	X			X	X	X	X		X	X		The residues are black so FTIR is not possible
N—H	3500–3300	Stretch	X			X	X	X	X		X	X		
	1485–1390	Stretch				X	X							
H—CH_2	3000–2850	Stretch	X	X				X	X		X	X		
C—CH_2—C	2950–2800	Asymetrical stretch	X	X	X				X			X		
C—CH—C	2930–2800	Stretch	X	X	X			X			X			
C═N	2400–2200	Stretch	X	X	X									
C═O	1850–1700	Stretch			X									
C═O Acid	1750–1650	Stretch	X	X	X			X	X		X	X		
C═O Amide	1700–1550	Stretch	X	X	X			X			X			
C═C aromatic	1660–1580	Stretch			X				X	X		X	X	
C═N aromatic	1660–1480	Stretch												
C—OH acid	1440–1395	Stretch	X	X	X			X	X		X	X		
CH_3—$CRRR^-$	1385–1370	Symmetrical deformation	X	X	X			X	X		X	X		
C—O—C aromatic and alphatic	1300–1050	Stretch	X	X	X			X	X		X	X		
P═O	1350–1150	Stretch				X	X							
P—OP	1100–800	Stretch				X	X	X			X			
P—OH	1030	Stretch				X	X	X	X		X	X		
P—O—C	1300–1100	Stretch								X			X	

T = temperature. At T > 370°C, the residues were black, so FTIR spectroscopy was not possible.

differences can be detected between the two crystalline forms.

The authors thank S. Seguro, O. Dobosz and L. Pankewitch (Centre de Recherche et d'Etude sur les Procédés d'Ignifugation des Matériaux), M. Vandewalle, G. Aiello, and B. Revel (Laboratoire des Procédés d'Elaboration de Revêtements Fonctionnels), and B. Castel (Institut Français du Textile et de l'Habillement) for their helpful technical assistance.

References

1. Dubois, A.; Rumeau, P. Internal Paper; Institut Français du Textile et de l'Habillement: Villeneuve d'Ascq, France, 1996.
2. Whistenant, J. L. Proceedings of Glo-Tex International, Atlanta, GA, Sept 2002; INDA, Association of the Nouwoven Fabrics Industry, Cary, N.C., p 490.
3. Grassie, N.; Zulfiqar, M. Dev Polym Stab 1979, 1, 197.
4. Camino, G. In Actes du 1er Colloque Francophone sur l'Ignifugation des Polymères; Martel, J., Ed.; Saint-Denis, France, 1985.
5. Vandersall, H. L. J Fire Flammability 1971, 2, 97.
6. Siat, C.; Bourbigot, S.; Le Bras, M. Rec Adv Flame Retardancy Polym Mater 1996, 7, 318.
7. Bugajny, M.; Le Bras, M.; Bourbigot, S. Rec Adv Flame Retardancy Polym Mater 1999, 10, 196.
8. Almeras, X.; Dabrowski, F.; Le Bras, M.; Poutch, F.; Bourbigot, S.; Marosi, G.; Anna, P. Polym Degrad Stab 2002, 77, 305.
9. Le Bras, M.; Bourbigot, S. Am Chem Soc Symp Ser 2001, 797, 136.
10. Drevelle, C.; Lefebvre, J.; Duquesne, S.; Le Bras, M.; Poutch, F.; Vouters, M.; Magniez, C. Polym Degrad Stab, to be published.
11. Camino, G.; Luda, M. P. In Fire Retardancy of Polymers: The Use of Intumescence; Le Bras, M.; Camino, G.; Bourbigot, S.; Delobel, R., Eds.; Royal Society of Chemistry: London, 1998; p 48.
12. Shen, C. Y.; Stahlheber, N. E.; Dyroff, D. R. J Am Chem Soc 1969, 91, 62.
13. Futterer, T.; Nagerl, H. D.; Gotzman, K. Presented at the 13th Annual BCC Conference on Flame Retardancy, Stamford, CT, June 2002.
14. Bugajny, M.; Bourbigot, S.; Le Bras, M.; Delobel, R. Polym Int 1999, 48, 264.
15. Bourbigot, S.; Le Bras, M.; Delobel, R. Carbon 1995, 33, 283.
16. Svehla, G., Ed.; Elsevier: Amsterdam, 1976.
17. McKee, D. W.; Spiro, C. L.; Lamby, E. J. Carbon 1984, 22, 285.
18. Duquesne, S.; Delobel, R.; Le Bras, M.; Camino, G. Polym Degrad Stab 2002, 77, 333.
19. Bugajny, M.; Le Bras, M.; Bourbigot, S.; Delobel, R. Polym Degrad Stab 1999, 64, 157.
20. McNeill, I. C.; Sadeghi, S. M. T. Polym Degrad Stab 1990, 29, 233.
21. McGaugh, M. C.; Kottle, S. Polym Lett 1967, 5, 817.
22. Eisenberg, A.; Yokoyama, T.; Sambalido, E. J Polym Sci Part A-1: Polym Chem 1969, 7, 1717.
23. Fyfe, C. A.; McKinnon, M. S. Macromolecules 1986, 19, 1909.
24. Maurer, J. J.; Eustace, D. J.; Ratcliffe, C. T. Macromolecules 1987, 20, 196.
25. Cameron, G. G.; Kane, D. R. Makromol Chem 1968, 113, 75.
26. Cameron, G. G.; Kane, D. R. Polymer 1968, 9, 461.
27. Barlow, A.; Lehrle, R. S.; Robb, J. C.; Sunderland, D. Polymer 1967, 8, 537.
28. McGaugh, M. C.; Kottle, S. J Polym Sci Part A-1: Polym Chem 1968, 6, 1243.
29. Maurer, J. J.; Harvey, G. D. Thermochim Acta 1987, 121, 295.
30. Leung, W. M.; Axelson, D. E.; Van Dyke, J. D. J Polym Sci Part A: Polym Chem 1987, 25, 1825.
31. Rafalko, J. J. J Polym Sci Polym Phys Ed 1984, 22, 1211.
32. Xue, T. J.; McKinney, M. A.; Wilkie, C. A. Polym Degrad Stab 1997, 58, 193.
33. Cameron, G. G.; Kane, D. R. Makromol Chem 1967, 109, 194.